

Supporting Information

Discovery of *N*-phenyl-4-(thiazol-5-yl)pyrimidin-2-amine Aurora Kinase Inhibitors

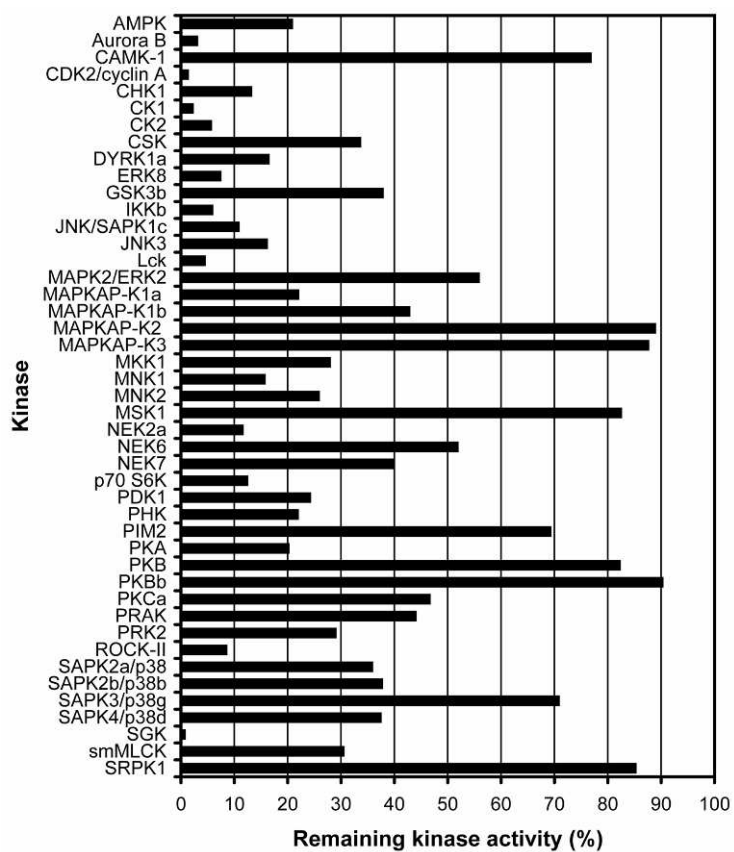
Shudong Wang,[†] Carol A. Midgley, Frederic Scaërou, Joanna B. Grabarek, Gary Griffiths, Wayne Jackson, George Kontopidis,[†] Steven J. McClue, Campbell McInnes,[†] Christopher Meades, Mokdad Mezna, Andy Plater, Iain Stuart, Mark P. Thomas, Gavin Wood, Rosemary G. Clarke, David G. Blake, Daniella I. Zheleva,^{} David P. Lane, Robert C. Jackson, David M. Glover, and Peter M. Fischer^{†,*}*

Cyclacel Limited, 1 James Lindsay Place, Dundee DD1 5JJ, Scotland, UK

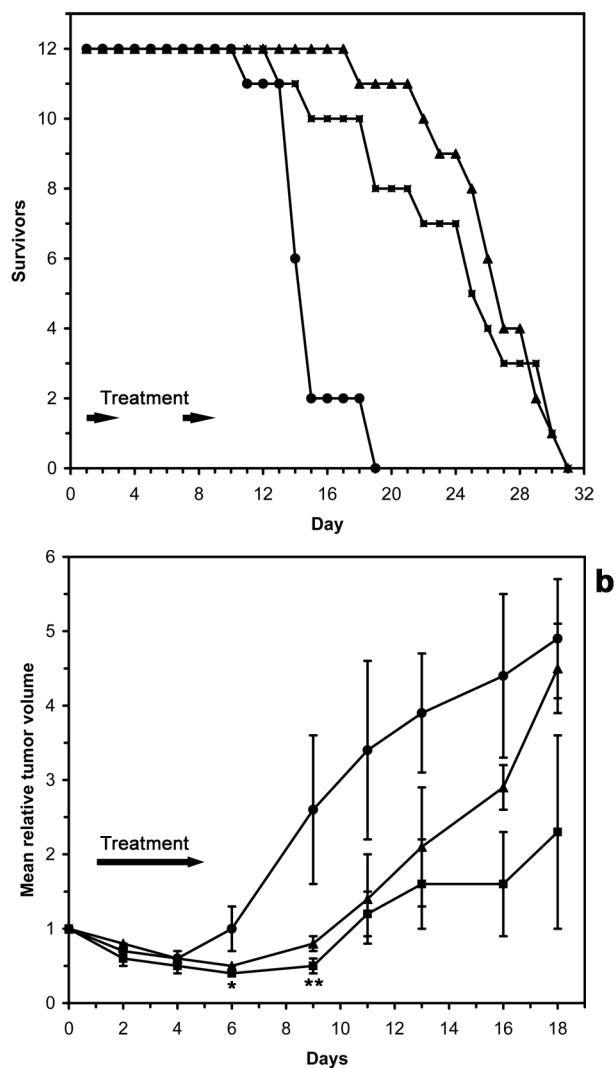
<u>Table of Contents</u>	<u>Page</u>
Supporting Figure 1. Kinase inhibitory activity of compound 18	S2
Supporting Figure 2. Activity of compound 18 in tumor models	S3
Synthesis and Characterization of Compounds 7h , 11–17 , and 19–24	S4
Biopharmaceutical Profiling	S7
Rat Pharmacokinetics	S7
Cell Viability Assay	S7
Murine P388/D1 Leukemia Model	S7
NCI-H460 Xenograft	S7
X-Ray Crystallography	S8
Molecular Modeling	S8
Supplementary References	S8

[†] Current addresses. For C.McI.: South Carolina College of Pharmacy, CLS 514, 715 Sumter St., University of South Carolina, Columbia, SC 29208, USA. For G.K.: Biochemistry Laboratory, Veterinary School, University of Thessaly, Karditsa 43100, Greece. For S.W. and P.M.F.: School of Pharmacy and Centre for Biomolecular Sciences, University of Nottingham, University Park, Nottingham NG7 2RD, UK.

* To whom correspondence should be addressed. For D.I.Z. (Cyclacel): phone, +44-1382-206062; E-mail: dzheleva@cyclacel.com. For P.M.F. (chemistry): phone, +44-115-8466242; E-mail: peter.fischer@nottingham.ac.uk.



Supporting Figure 1. Kinase inhibitory activity of compound **18**. The assays were carried out in the presence of 5 μ M compound **18** and the ATP concentrations were the $K_{M, ATP}$ for the individual kinases.



Supporting Figure 2. Activity of compound **18** in tumor models. Murine P388/D1 model (a). Tumor-bearing animals were dosed orally twice daily on days 1–3 and 7–9 with: vehicle control (●), 45 mg/kg/dose **18** (■), or 67 mg/kg/dose **18** (▲). Murine NCI-H460 non-small cell lung cancer xenograft model (b). Starting on day 1 and for 5 days, groups of ten animals were administered orally: vehicle control (●), 75 mg/kg/dose **18** once daily (▲), or 100 mg/kg/dose **18** once daily (■). Standard error means (SEM) are indicated and growth reduction compared to the vehicle control was statistically significant for measurements on days 6 and 9 (*, $P < 0.05$; **, $P < 0.001$) as shown.

Synthesis and Characterization of Compounds 7h, 11 – 17, and 19 – 24

1-(4-(4-Aminophenyl)piperazin-1-yl)ethanone (7h). 1-(4-(4-nitrophenyl)piperazin-1-yl)-ethanone **6h** was prepared as described:¹ Orange solid. ¹H-NMR (DMSO-*d*₆): δ 2.15 (s, 3H, CH₃), 3.26 (dd, 2H, *J* = 5.5 Hz, CH₂), 3.30 (dd, 2H, *J* = 5.5 Hz, CH₂), 3.66 (dd, 2H, *J* = 5.5 Hz, CH₂), 3.80 (dd, 2H, *J* = 5.5 Hz, CH₂), 7.20 (d, 1H, *J* = 5.0 Hz, Ph-H), 7.40 (d, 1H, *J* = 5.0 Hz, Ph-H), 7.70 (d, 1H, *J* = 5.0 Hz, Ph-H), 7.72 (s, 1H, Ph-H). Treatment of a solution of **6h** in AcOH/EtOH (1:2, v/v) with Fe (3 eq) and heating at 80 °C for 3 h afforded the title compound **7h** as a yellow oil in 90% yield. ¹H-NMR (DMSO-*d*₆): δ 2.07 (s, 3H, CH₃), 3.08 (m, 4H, CH₂), 3.55 (m, 2H, CH₂), 3.72 (m, 2H, CH₂), 6.22 (d, 1H, *J* = 8.0 Hz, Ph-H), 6.25 (s, 1H, Ph-H), 6.32 (d, 1H, *J* = 8.0 Hz, Ph-H), 7.00 (dd, 1H, *J* = 8.0 Hz, Ph-H).

N¹-(4-(2,4-Dimethylthiazol-5-yl)pyrimidin-2-yl)-N⁴-methylbenzene-1,4-diamine (11). By condensation between enaminone **4a** and phenylguanidine **8c**. Yellow crystals (68%); mp 155–156 °C. Anal. RP-HPLC: *t*_R = 19.9 min (5–60% MeCN; purity 100%). ¹H-NMR (DMSO-*d*₆): δ 2.59 (s, 3H, CH₃), 2.63 (s, 3H, CH₃), 2.66 (m, 3H, CH₃), 5.32 (bs, 1H, NH), 6.50 (d, 1H, *J* = 8.5 Hz, Ph-H), 6.91 (d, 1H, *J* = 5.5 Hz, Py-H), 7.42 (d, 1H, *J* = 8.5 Hz, Ph-H), 8.38 (d, 1H, *J* = 5.5 Hz, Py-H), 9.16 (s, 1H, NH). ¹³C-NMR (DMSO-*d*₆): δ 18.54, 19.65, 30.92, 107.86, 112.23, 122.09, 129.90, 146.27, 152.31, 152.31, 158.51, 159.58, 160.76, 166.77. MS (ESI⁺): *m/z* 312.42 [M+H]⁺. Anal. (C₁₆H₁₇N₅S) C, H, N.

N¹-(4-(2,4-Dimethylthiazol-5-yl)pyrimidin-2-yl)benzene-1,4-diamine (12). By condensation between enaminone **4a** and phenylguanidine **8d**. Yellow crystals (82%); mp 206–208 °C. Anal. RP-HPLC: *t*_R = 16.0 min (5–60% MeCN; purity 100%). ¹H-NMR (DMSO-*d*₆): δ 2.59 (s, 3H, CH₃), 2.62 (s, 3H, CH₃), 4.75 (bs, 2H, NH₂), 6.51 (d, 1H, *J* = 8.5 Hz, Ph-H), 6.91 (d, 1H, *J* = 4.9 Hz, Py-H), 7.31 (d, 2H, *J* = 7.8 Hz, Ph-H), 8.38 (d, 1H, *J* = 5.4 Hz, Py-H), 9.11 (s, 1H, NH). ¹³C-NMR (DMSO-*d*₆): δ 18.54, 19.64, 107.86, 114.55, 122.15, 129.97, 131.68, 144.58, 152.31, 158.52, 159.59, 160.79, 166.77. MS (ESI⁺): *m/z* 298.03 [M+H]⁺. Anal. (C₁₅H₁₅N₅S) C, H, N.

4-(2,4-Dimethylthiazol-5-yl)-N-(3,4,5-trimethoxyphenyl)pyrimidin-2-amine (13). By condensation between enaminone **4a** and phenylguanidine **8e**. Yellow solid (76%). Anal. RP-HPLC: *t*_R = 14.1 min (10–70% MeCN, purity 99%). ¹H-NMR (DMSO-*d*₆): δ 2.07 (s, 6H, CH₃), 3.62 (s, 3H, CH₃), 3.79 (s, 6H, CH₃), 7.08 (d, 1H, *J* = 5.0 Hz, Py-H), 7.18 (s, 2H, Ph-H), 8.51 (d, 1H, *J* = 5.0 Hz, Py-H), 9.51 (s, 1H, NH). MS (ESI⁺) *m/z* 373.34 [M+H]⁺. Anal. (C₁₈H₂₀N₄O₃S) C, H, N.

N,4-Dimethyl-5-(2-(3,4,5-trimethoxyphenylamino)pyrimidin-4-yl)thiazol-2-amine (14). By condensation between enaminone **4c** and phenylguanidine **8e**. Yellow solid (86%). Anal. RP-HPLC: *t*_R = 11.1 min (10–70% MeCN, purity 99%). ¹H-NMR (DMSO-*d*₆): δ 2.46 (s, 3H, CH₃), 3.61 (s, 3H, CH₃), 3.61 (s, 3H, CH₃), 3.81 (s, 6H, CH₃), 6.90 (d, 1H, *J* = 5.5 Hz, Py-H), 7.17 (s, 2H, Ph-H), 8.32 (d, 1H, *J* = 5.5 Hz, Py-H), 9.28 (s, 1H, NH). MS (ESI⁺) *m/z* 388.33 [M+H]⁺. Anal. (C₁₈H₂₁N₅O₃S) C, H, N.

N-Ethyl-4-methyl-5-(2-(3,4,5-trimethoxyphenylamino)pyrimidin-4-yl)thiazol-2-amine (15). By condensation between enaminone **4d** and phenylguanidine **8e**. Yellow solid (69%). Anal. RP-HPLC: *t*_R = 12.1 min (10–70% MeCN, purity 99%). ¹H-NMR (DMSO-*d*₆): δ 1.17 (t, 3H, *J* = 7.5 Hz, CH₃), 2.45 (s, 3H, CH₃), 3.61 (s, 3H, CH₃), 3.80 (s, 6H, CH₃), 6.90 (d, 1H, *J* = 6.0 Hz, Py-H), 7.16 (s, 2H, Ph-H), 8.13 (m, 1H, NH), 8.32 (d, 1H, *J* = 5.5 Hz, Py-H), 9.27 (s, 1H, NH). MS (ESI⁺) *m/z* 402.37 [M+H]⁺. Anal. (C₁₉H₂₃N₅O₃S) C, H, N.

***N*-(4-(4-(2-(Ethylamino)-4-methylthiazol-5-yl)pyrimidin-2-ylamino)benzyl)acetamide (16).** By condensation between enaminone **4d** and phenylguanidine **8f**. Pale solid (57%); mp 210–212 °C. Anal. RP-HPLC: t_R = 12.3 min (5–60% MeCN; purity 92%). ¹H-NMR (DMSO-*d*₆): δ 1.28 (t, 3H, *J* = 7.0 Hz, CH₃), 1.99 (s, 3H, CH₃), 2.52 (s, 3H, CH₃), 3.36 (q, 2H, *J* = 7.0, 14.5 Hz, CH₂), 4.31 (s, 2H, CH₂) 6.9 (d, 1H, *J* = 5.5 Hz, Py-H), 7.22 (d, 2H, *J* = 8.5 Hz, Ph-H), 7.66 (d, 2H, *J* = 9.0 Hz, Ph-H), and 8.25 (d, 1H, *J* = 5.5 Hz, Py-H). ¹³C-NMR (DMSO-*d*₆): δ 14.95, 19.33, 23.27, 42.49, 60.41, 107.34, 118.30, 119.25, 128.23, 132.80, 140.06, 152.85, 158.24, 159.22, 160.10, 168.92, 169.64. HRMS (ESI⁺): *m/z* 383.16491 [M+H]⁺. Anal. (C₁₉H₂₂N₆OS) C, H, N.

4-(2,4-Dimethylthiazol-5-yl)-*N*-(4-morpholinophenyl)pyrimidin-2-amine (17). By condensation between enaminone **4a** and phenylguanidine **8g**. Pale solid (74%); mp 117–120 °C. ¹H-NMR (DMSO-*d*₆): δ 2.61 (s, 3H, CH₃), 2.63 (s, 3H, CH₃), 3.04 (m, 4H, CH₂), 3.73 (m, 4H, CH₂), 6.91 (d, 1H, *J* = 9.5 Hz, Ph-H), 6.99 (d, 2H, *J* = 5.5 Hz, Py-H), 7.61 (d, 2H, *J* = 9.5 Hz, Ph-H), 8.44 (d, 1H, *J* = 5.0 Hz, Py-H). ¹³C-NMR (DMSO-*d*₆): δ 18.56, 19.68, 49.94, 66.88, 108.39, 116.25, 120.98, 121.01, 133.36, 146.95, 152.47, 159.67, 159.68, 160.50, 166.92. MS (ESI⁺): *m/z* 368.00 [M+H]⁺. Anal. (C₁₉H₂₁N₅OS), C, H, N.

***N*,4-Dimethyl-5-(2-(4-morpholinophenylamino)pyrimidin-4-yl)thiazol-2-amine (19).** By condensation between enaminone **4c** and phenylguanidine **8g**. Pale solid (81%); mp 286–289 °C. Anal. RP-HPLC: t_R = 10.8 min (0–60% MeCN; purity 99%). ¹H-NMR (DMSO-*d*₆): δ 2.46 (s, 3H, CH₃), 2.85 (m, 3H, CH₃), 3.03 (m, 4H, CH₂), 3.73 (m, 4H, CH₂), 6.81 (d, 1H, *J* = 5.5 Hz, Py-H), 6.87 (d, 2H, *J* = 8.5 Hz, Ph-H), 7.61 (d, 2H, *J* = 8.5 Hz, Ph-H), 8.00 (bs, 1H, NH), 8.26 (d, 1H, *J* = 5.5 Hz, Py-H), 9.17 (bs, 1H, NH). ¹³C-NMR (DMSO-*d*₆): δ 19.32, 31.44, 50.03, 66.89, 106.86, 116.27, 120.74, 120.78, 133.83, 146.66, 152.69, 158.27, 159.28, 160.30, 169.88. MS (ESI⁺): *m/z* 383.13 [M+H]⁺. Anal. (C₁₉H₂₂N₆OS) C, H, N.

***N*-Ethyl-4-methyl-5-(2-(4-morpholinophenylamino)pyrimidin-4-yl)thiazol-2-amine (20).** By condensation between enaminone **4d** and phenylguanidine **8g**. Pale solid (73%); mp 253–254 °C. Anal. RP-HPLC: t_R = 9.77 min (10–70% MeCN; purity 100%). ¹H-NMR (DMSO-*d*₆): δ 1.16 (t, 3H, *J* = 3.5 Hz, CH₃), 2.45 (s, 3H, CH₃), 3.02 (m, 4H, CH₂), 3.28 (m, 2H, CH₂), 3.73 (m, 4H, CH₂), 6.81 (d, 1H, *J* = 6.0 Hz, Py-H), 6.87 (d, 2H, *J* = 8.5 Hz, Ph-H), 7.61 (d, 2H, *J* = 8.5 Hz, Ph-H), 8.05 (m, 1H, NH), 8.26 (d, 1H, *J* = 6.0 Hz, Py-H), 9.17 (bs, 1H, NH). ¹³C-NMR (DMSO-*d*₆): δ 15.00, 19.33, 50.04, 66.89, 106.89, 116.26, 118.40, 120.73, 133.84, 146.64, 152.61, 158.22, 159.28, 160.29, 168.91. MS (ESI⁺): *m/z* 396.98 [M+H]⁺. Anal. (C₂₀H₂₄N₆OS) C, H, N.

1-(4-(4-(4-(2-Amino-4-methylthiazol-5-yl)pyrimidin-2-ylamino)phenyl)piperazin-1-yl)ethanone (21). By condensation between enaminone **4b** and phenylguanidine **8h**. Light yellow solid (58%); mp 267–269 °C. Anal. RP-HPLC: t_R = 7.21 min (10–70% MeCN; purity 100%). ¹H-NMR (DMSO-*d*₆): δ 2.42 (s, 3H, CH₃), 3.00 (m, 2H, CH₂), 3.07 (m, 2H, CH₂), 3.29 (s, 3H, CH₃), 3.58 (m, 4H, CH₂), 6.81 (d, 1H, *J* = 5.5 Hz, Py-H), 6.89 (d, 2H, *J* = 9.0 Hz, Ph-H), 7.46 (s, 2H, NH₂), 7.62 (d, 2H, *J* = 8.0 Hz, Ph-H), 8.26 (d, 1H, *J* = 5.5 Hz, Py-H), 9.19 (bs, 1H, NH). ¹³C-NMR (DMSO-*d*₆): δ 19.10, 21.90, 41.49, 46.31, 49.97, 50.40, 107.01, 117.19, 118.90, 120.69, 134.11, 146.38, 152.43, 158.26, 159.33, 160.38, 168.94, 169.42. MS (ESI⁺): *m/z* 410.52 [M+H]⁺. Anal. (C₂₀H₂₃N₇OS) C, H, N.

1-(4-(4-(4-(4-Methyl-2-(methylamino)thiazol-5-yl)pyrimidin-2-ylamino)phenyl)piperazin-1-yl)ethanone (22). By condensation between enaminone **4c** and phenylguanidine **8h**. Yellow solid (69%); mp 230–231 °C. Anal. RP-HPLC: t_R = 8.8 min (10–70% MeCN; purity 97%). ¹H-NMR (DMSO-*d*₆): δ 2.85 (s, 3H, CH₃), 2.99 (m, 2H, CH₂), 3.07 (m, 2H, CH₂), 3.16 (s, 3H, CH₃), 3.27 (s, 3H, CH₃), 3.57 (m, 4H, CH₂), 6.82 (d, 1H, *J* =

6.0 Hz, Py-H), 6.89 (d, 2H, $J = 9.0$ Hz, Ph-H), 7.61 (d, 2H, $J = 9.0$ Hz, Ph-H), 8.26 (d, 1H, $J = 5.5$ Hz, Py-H), 9.18 (s, 1H, NH). $^{13}\text{C-NMR}$ (DMSO- d_6): δ 14.79, 21.46, 21.91, 41.50, 46.32, 49.29, 60.46, 117.26, 120.72, 122.02, 134.11, 145.35, 146.41, 152.73, 160.28, 164.55, 165.93, 168.94, 171.05. MS (ESI $^+$): m/z 424.07 [M+H] $^+$. Anal. (C $_{21}$ H $_{25}$ N $_7$ OS) C, H, N.

1-(4-(4-(4-(2,4-Dimethylthiazol-5-yl)pyrimidin-2-ylamino)phenyl)piperazin-1-yl)ethanone (23). By condensation between enaminone **4a** and phenylguanidine **8h**. Yellow solid (67%); mp 151-153 °C. Anal. RP-HPLC: $t_R = 12.1$ min (10–70% MeCN; purity 100%). $^1\text{H-NMR}$ (DMSO- d_6): δ 2.61 (s, 3H, CH $_3$), 2.64 (s, 3H, CH $_3$), 3.01 (t, 2H, $J = 5.5$ Hz, CH $_2$), 3.07 (t, 2H, $J = 5.0$ Hz, CH $_2$), 3.34 (s, 3H, CH $_3$), 3.57 (m, 4H, CH $_2$), 6.93 (d, 2H, $J = 8.5$ Hz, Ph-H), 6.99 (d, 1H, $J = 5.0$ Hz, Py-H), 7.62 (d, 2H, $J = 9.5$ Hz, Ph-H), 8.44 (d, 1H, $J = 5.5$ Hz, Py-H), 9.43 (s, 1H, NH). $^{13}\text{C-NMR}$ (DMSO- d_6): δ 18.57, 19.68, 21.90, 41.46, 46.30, 49.88, 50.31, 108.43, 117.18, 120.95, 131.61, 133.64, 146.69, 158.56, 159.72, 160.48, 166.94, 168.93. MS (ESI $^+$): m/z 409.31 [M+H] $^+$. Anal. (C $_{21}$ H $_{24}$ N $_6$ OS) C, H, N.

4-(2,4-Dimethylthiazol-5-yl)-N-(4-(4-(methylsulfonyl)piperazin-1-yl)phenyl)pyrimidin-2-amine (24). By condensation between enaminone **4a** and phenylguanidine **8i**. Yellow solid (62%). $^1\text{H-NMR}$ (CDCl $_3$): δ 2.69 (s, 3H, CH $_3$), 2.71 (s, 3H, CH $_3$), 2.84 (s, 3H, CH $_3$), 3.26 (t, 4H, $J = 5.1$ Hz, CH $_2$), 3.41 (t, 4H, $J = 5.1$ Hz, CH $_2$), 6.91 (d, 1H, $J = 5.1$ Hz, Py-H), 6.98 (d, 2H, $J = 8.8$ Hz, Py-H), 7.10 (bs, 1H, NH), 7.56 (d, 2H, $J = 8.8$ Hz, Ph-H), 8.38 (d, 1H, $J = 5.1$ Hz, Ph-H). MS (ESI $^+$) m/z 446.00 [M+H] $^+$. Anal. (C $_{20}$ H $_{24}$ N $_6$ O $_2$ S $_2$) C, H, N.

Biopharmaceutical Profiling. Test compound partitioning between octanol and aqueous buffer was carried out using the shake-flask method.² Compound pK_a values were determined using a pH-metric titration method (GLpKa; Sirius).³ Aqueous solubility was assessed by turbidimetric measurements.⁴ Apparent permeability coefficients were measured using a Caco-2 cell layer assay.⁵ In vitro phase-I liver metabolism was assessed by disappearance of parent compound (LC-MS quantitation) from a preparation of rat liver microsomes.⁶ Rat plasma protein binding was determined in an equilibrium dialysis assay.⁷ hERG inhibition was assessed using automated patch clamp electrophysiology measurement in CHO-hERG cells.⁸

Rat Pharmacokinetics. The PK parameters for test compounds were determined in male Wistar rats. For each compound, 3 rats were dosed either by intravenous bolus injection or by oral gavage. Dose volume was 10 mL/kg for oral gavage administration and 12 mL/kg for intravenous administration (1mL/min). Three serum samples were collected from each rat by jugular vein cannulation at 0, 5, 15, and 30 min, 1, 2, 4, and 6 h following i.v. dosing; and at 0, 0.5, 1, 2, 4, 6, 8, and 24 h after p.o. dosing. All blood samples were centrifuged immediately following collection. The plasma was harvested and stored at $-20\text{ }^{\circ}\text{C}$ until analysis. The samples were analyzed by LC-MS/MS methods. The PK parameters were derived by noncompartmental methods using WinNonlin 5.2 software program (Pharsight). The oral bioavailability (% F) was calculated by taking the ratio of dose-normalized AUC values from oral versus i.v. dosing.

Cell Viability Assay. Inhibition of cell growth was measured by a standard MTT (thiazolyl blue; 3-[4,5-dimethylthiazol-2-yl]-2,5-diphenyltetrazolium bromide) assay using a panel of tumor cell lines.⁹ Briefly: cells were seeded (2,500–5,000 cells/well) in 96-well plates and allowed to attach for ~ 24 h. Cells were incubated with test compounds for 96 h in DMEM medium containing 10% fetal bovine serum. Cells were treated with a range of compound concentrations in triplicate to generate dose-response curves. The compound concentration required to inhibit 50% of cell growth (IC_{50}) was determined using nonlinear regression analysis.

Murine P388/D1 Leukemia Model. Female Balb/c \times DBA/2J F1 mice were implanted intraperitoneally with 2.1×10^5 P388/D1 leukemia cells on day 0. Starting on day 1 the animals were administered compound **18** by oral gavage at the indicated doses (0.1 mL / 10 g body weight) twice a day on days 1–3 and 7–9. The effectiveness of treatment was assessed by comparison of the median post-inoculation lifespan (ILS) of each group of treated mice with that of the vehicle control group. The ratio of ILS values for the treated versus the control groups was expressed as a percentage value (% ILS) and used as an indicator of relative efficacy.

NCI-H460 Xenograft. Human NCI-H460 non-small cell lung tumor cells were harvested from sub-confluent cultures grown in vitro and the number of viable cells was determined. Cells were then resuspended in sterile PBS at a concentration of ca. 7×10^7 cells/mL. Nude (athymic) mice were injected subcutaneously in the right flank with approximately 7×10^6 cells. When measurable tumors had established (80-100 mm³), animals were assigned into the treatment and the control groups with 10 mice per group. Tumor size was measured at least twice weekly. Animals were terminated at any time during the study if the tumor size became excessive or any adverse effects were noted. The treatments were administered orally, by gavage, daily, starting on day 1, and continuing for 5 days. In the control group, animals were treated with the vehicle orally, by gavage, once a day starting on day 1, and continuing for 5 days. The tumor dimensions measured over the period of the study were recorded. Calculations of relative tumor volumes and plots of mean tumor growth curves were

performed. The relative tumor volume data from each group were compared using a one-way analysis of variance (ANOVA) and statistical significance was determined using a Dunnett's *t*-test.

X-Ray Crystallography. Protein production and crystallography methods have been described previously.¹⁰ Data were collected at the Grenoble (France) synchrotron facilities using an ADSC Quantum4 CCD detector. Data processing was carried out using the programs MOSFLM¹¹ and SCALA¹² from the CCP4 program suite.¹³ The **18**-CDK2-cyclin A complex structure was solved by molecular replacement using MOLREP¹⁴ and PDB entry 1OKV as the search model. ARP/wARP¹⁵ was used for initial density interpretation and the addition of water molecules. REFMAC¹⁴ was used for structural refinement. A number of rounds of refinement and model building with the program Quanta (Accelrys, San Diego, USA) were carried out. Coordinates of the **18**-CDK2-cyclin A complex structure have been deposited with the RCSB under accession code 2UUE.

Molecular Modeling. The structure coordinates of aurora A were obtained from the RCSB (accession code 1OL5). Inhibitors were docked into the ATP site using the Affinity program (Accelrys, San Diego, CA). The binding site was defined as an 8 Å radius from the centre of a ligand binding mode. The molecular docking routine adopted, which incorporated a full molecular mechanics approach, allows for flexibility both in the ligand and in the side chains and backbone of the receptor (the positions of the C^α atoms were fixed during the simulation). The calculation was performed using the CVFF force field in a two-step process using an implicitly derived solvation model and geometric hydrogen bond restraints. For the initial phase of the calculation, the inhibitor was minimized into the ATP cleft, using a simple non-bonded method where the Coulombic and van der Waals terms were scaled to zero and 0.1, respectively. The subsequent refinement phase involved conformational sampling using molecular dynamics calculated over 5 ps in 100 fs stages, where the temperature was scaled from 500 K to 300 K. The calculation was completed by a final minimization over 1,000 steps using the Polak-Ribiere Conjugate Gradient method. The docked structures were ranked energetically (using the in-house developed programs Calsor and Calsorcont, values reported in kcal/mol) and by consistency of the non-bonded contacts with the CDK binding pose and known kinase interactions, in order to determine the most representative binding mode.

Supplementary References

1. Orus, L.; Martinez, J.; Perez, S.; Oficialdegui, A. M.; del Castillo, J. C.; Mourelle, M.; Lasheras, B.; del Rio, J.; Monge, A. New 3-[4-(3-substituted phenyl)piperazin-1-yl]-1-(benzo[b]thiophen-3-yl)-propanol derivatives with dual action at 5-HT_{1A} serotonin receptors and serotonin transporter as a new class of antidepressants. *Pharmazie* **2002**, *57*, 515-518.
2. Dearden, J. C. Partitioning and lipophilicity in quantitative structure-activity relationships. *Environ. Health Persp.* **1985**, *61*, 203-228.
3. Comer, J. E. A. High-throughput measurement of log D and pK_a. *Methods Principles Med. Chem.* **2003**, *18*, 21-45.
4. Brooker, P. J.; Ellison, M. Determination of the water solubility of organic compounds by a rapid turbidimetric method. *Chem. Ind.* **1974**, 285-287.

5. Gan, L.-S. L.; Thakker, D. R. Applications of the Caco-2 model in the design and development of orally active drugs: elucidation of biochemical and physical barriers posed by the intestinal epithelium. *Adv. Drug Delivery Rev.* **1997**, *23*, 77-98.
6. Houston, J. B.; Carlile, D. J. Prediction of hepatic clearance from microsomes, hepatocytes, and liver slices. *Drug Metabol. Rev.* **1997**, *29*, 891-922.
7. Kariv, I.; Cao, H.; Oldenburg, K. R. Development of a high throughput equilibrium dialysis method. *J. Pharm. Sci.* **2001**, *90*, 580-587.
8. Sorota, S.; Zhang, X. S.; Margulis, M.; Tucker, K.; Priestley, T. Characterization of a hERG screen using the IonWorks HT: comparison to a hERG rubidium efflux screen. *Assay Drug Dev Technol* **2005**, *3*, 47-57.
9. Haselsberger, K.; Peterson, D. C.; Thomas, D. G.; Darling, J. L. Assay of anticancer drugs in tissue culture: comparison of a tetrazolium-based assay and a protein binding dye assay in short-term cultures derived from human malignant glioma. *Anti Cancer Drugs* **1996**, *7*, 331-338.
10. Andrews, M. J. I.; Kontopidis, G.; McInnes, C.; Plater, A.; Innes, L.; Cowan, A.; Jewsbury, P.; Fischer, P. M. REPLACE: A Strategy for Iterative Design of Cyclin-Binding Groove Inhibitors. *ChemBioChem* **2006**, *7*, 1909-1915.
11. Leslie, A. G. W. Recent changes to the MOSFLM package for processing film and image plate data. *Joint CCP4 + ESF-EAMCB Newsletter on Protein Crystallography* 1992.
12. Evans, P. R. In *Data reduction*, Proceedings of CCP4 Study Weekend on Data Collection & Processing, 1993; 1993; pp 114-122.
13. Project, C. C. The CCP4 suite: programs for protein crystallography. *Acta Crystallogr.* **1994**, *D50*, 760-763.
14. Murshudov, G. N.; Vagin, A. A.; Dodson, E. J. Refinement of macromolecular structures by the maximum-likelihood method. *Acta Crystallogr D Biol Crystallogr* **1997**, *53*, 240-255.
15. Lamzin, V. S., and Wilson, K.S. Automated refinement for protein crystallography. *Methods Enzymol.* **1997**, *277*, 269-305.